Behavioral Neuroscience

Amyloid-Beta Accumulation, Neurogenesis, Behavior, and the Age of Rats

Russell M. Church, Miles C. Miller, David Freestone, Catharine Chiu, Doreen P. Osgood, Jason T. Machan, Arthur A. Messier, Conrad E. Johanson, and Gerald D. Silverberg

Online First Publication, May 19, 2014. http://dx.doi.org/10.1037/a0036433

Behavioral Neuroscience

0735-7044/14/$12.00 DOI: 10.1037/a0036433

Amyloid-Beta Accumulation, Neurogenesis, Behavior, and the Age of Rats

Russell M. Church
Brown University

Miles C. Miller
Brown University and Warren Alpert Medical School

David Freestone
Brown University

Catharine Chiu, Doreen P. Osgood, Jason T. Machan, and Arthur A. Messier
Brown University and Warren Alpert Medical School

Conrad E. Johanson
Brown University

Gerald D. Silverberg
Brown University, Warren Alpert Medical School

The goals of this research were to describe age-related changes in brain biochemistry and behavior, and the relationships between them. The chronological ages of greatest change are particularly important for targeting interventions. In this experiment, 36 Fischer 344/Brown-Norway rats (3, 12, 20, and 30 months old) were trained in lever boxes on temporal discrimination tasks. The greatest response rate decrease and response pattern change occurred between 12 and 20 months. The biochemical results showed that amyloid-beta peptides (Aβ40 and Aβ42) increased with age. The endothelial expression of the Aβ influx transporter (RAGE) also increased, and the expression of Aβ efflux transporter (LPR-1) decreased, with age. The greatest change in the biochemical measures also were between 12 and 20 months. Twenty additional rats were analyzed for stem cell proliferation, and neurogenesis decreased with age, particularly between about 12 and 20 months. These early changes in brain, biochemistry, and behavior provide opportunity for new therapies or prophylaxis.

Keywords: aging, Alzheimer, amyloid, neurogenesis, behavior

Chronological aging is accompanied by changes in both brain and behavior. The primary purpose of this article is to describe some quantitative changes in biochemistry and behavior that occur in individual rats during chronological aging. This makes it possible to make age-related comparisons between biochemical and behavioral variables.

Rat models of brain and behavioral aging have used inbred, hybrid, and outbred strains in aging research. We used the Fischer F344/Brown-Norway (F344/BN) F1 hybrid that has a median life span of about three years (Turturro et al., 1999). The rat model has the advantage of a relatively short life expectancy compared with humans, and provides researchers with the opportunity to control environmental conditions for the analysis of age-related biochemical and behavioral changes. F344/BN rats were used because they are long-lived, compared with other strains of rats, relatively free of spontaneous neoplasia, and easily obtained at different ages from the NIA colony (Turturro et al., 1999). Reviews of the use of rats as models of human aging include Gallagher and Rapp (1997), Nadon (2007), van der Staay (2006), and van der Staay, Arndt, and Nordquist (2009).

For the study of human aging, the rat model is well established. Research with rats and humans often obtain similar age-related changes in biochemical and behavioral processes (Gallagher, Stocker, & Koh, 2011). The interactions between biochemical and behavioral processes are demonstrated by the studies of enriched environments (Wood, Glynn, & Morton, 2011), calorie restriction (Fontana & Klein, 2007), low stress (Boonstra, 2005), and exercise (Nocon et al., 2008). These studies have provided experimental manipulations that affect biochemistry and behavior, and that increase longevity.

Amyloid-beta peptide (Aβ) accumulates in the brain in normal aging in rats (Silverberg et al., 2010a) and humans (Price, Davis, Morris, & White, 1991), and it is a hallmark of Alzheimer's disease (AD). Rodent Aβ differs from the human version by three amino acid residues (Esler, Stimson, Jennings, et al., 1996). There-

Russell M. Church, Cognitive, Linguistic & Psychological Sciences, Brown University; Miles C. Miller, Department of Neurosurgery, Brown University and Warren Alpert Medical School; David Freestone, Cognitive, Linguistic & Psychological Sciences, Brown University; Catharine Chiu, and Doreen P. Osgood, Department of Neurosurgery, Brown University; Jason T. Machan, Biostatistics Core, Brown University; Arthur A. Messier, Department of Neurosurgery, Brown University and Warren Alpert Medical School; Conrad E. Johanson, Department of Neurosurgery, Brown University; Gerald D. Silverberg, Department of Neurosurgery, Brown University, and Warren Alpert Medical School.

Funding for the studies came from the Saunders Family Fund at the Neurosurgical Foundation at Brown University. We thank Virginia Hovanesian, Paul Monfils, Nancy L. Heath, and Renée Monahan for their technical contributions to these studies.

Correspondence concerning this article should be addressed to Russell M. Church, Department of Cognitive, Linguistic, and Psychological Sciences, Brown University, Box 1821, Providence, RI 02912. E-mail: Russell_Church@Brown.edu

fore, rat Aβ does not form the same fibrillar Aβ and beta-sheet structure, and is less toxic than human Aβ. Transgenic rodents overexpressing human Aβ are a better model for familial AD. However, rat Aβ does self-assemble into potentially toxic oligomeric forms that could harm neuronal synapses and neural stem cell proliferation, as does human Aβ (Esler, Stimson, Jennings, et al., 1996; Shruster, Eldar-Finkelman, Melamed, & Offen 2011; Walsh et al., 2002; Wicklund et al., 2010; Witton, Brown, Jones, & Randall 2010). We therefore wished to test whether the age-related accumulation of rodent Aβ had behavioral effects, and might serve as a model for age-related memory and cognitive impairment. The speed of mental processing decreases in normal aging and AD (Salthouse, 2000). In this article, the biochemical measures focus on Aβ accumulation and decreased Aβ clearance in aging (Silverberg et al., 2010a, 2010b), and on decreased number of new neural stem cells as a function of aging. We measured Aβ accumulation by ELISA, and we assessed the primary transporter expressions at the blood-brain barrier by immunohistochemistry (IHC). The primary Aβ efflux transporter is the low-density lipoprotein receptor-related protein 1 (LRP-1), and the primary Aβ influx transporter is the receptor for advanced glycation end products (RAGE or AGER). Adult neurogenesis was measured by 5-bromo-2′deoxyuridine (BrdU) labeling of the dentate gyrus (DG) and subventricular zone (SVZ) as a function of age. BrdU has become a useful tool for studying cell proliferation in both the developing (Nowakowski, Lewin, & Miller, 1989) and adult (Eriksson et al., 1998) nervous system. Neurogenesis is facilitated by some types of learning (Curlik & Shors, 2013; Gould, Beylin, Tanapat, Reeves, & Shors, 1999).

The behavioral changes focused on the speed, accuracy, and precision of performance and the speed and pattern of learning. These were measured by the behavior of the rats in timing tasks in lever boxes.

The same rats were used for obtaining brain Aβ concentrations, the BBB Aβ transporter expression data, and behavioral measures. This made it possible to examine (a) the relationship of the brain and behavioral variables to chronological age, (b) the relationship among different biochemical measures, and among different behavioral measures, and (c) the relationship between biochemical and behavioral measures.

Method

Subjects

Fifty-six Fischer 344/Brown-Norway (F344/BN) F1 male hybrid rats were delivered from the Harlan Laboratory at four ages (3, 12, 20, and 30 months). The number of rats at each age in each group is shown in Table 1. There were 14 rats at each age. They were housed in individual cages and handled daily. Two rats in the 30-month group died prior to the end of the experiment, and their data were not used. After daily handling and cognitive testing, 34 of the rats were euthanized by intraperitoneal (ip) pentobarbital (125 mg/kg), and were perfused with phosphate-buffered saline via left ventricular cardiac cannulation prior to brain removal for ELISA measurements of Aβ concentrations and immunohistochemical measures of receptor protein expression. Due to limitations on rat brain tissue, confirmatory western blotting could not be done on the behaviorally tested rats. Our prior publications, however, have shown a close correlation between semiquantitative immunostaining and western blot protein analysis (Silverberg et al., 2010a, 2010b). The other 20 F344/BN rats (five at each of the same four age groups) were used for neural stem cell proliferation counts, but were not behaviorally tested. All experiments were approved by the Institutional Animal Care and Use Committee (IACUC) at Rhode Island Hospital and at Brown University.

Table 1
Number of Rats in Three Groups and Four Ages

	Age				
Group	3	12	20	20	Sum
Group 1	6	6	6	6	24
Group 2	3	3	3	3	12
Group 3	5	5	5	5	20
Sum	14	14	14	14	56

Behavioral Testing

Apparatus. Twenty-four operant boxes (Med Associates, Inc., St. Albans, VT) were used. Each box contained a retractable lever, a feeder, a speaker, a programmable audio generator, a house light, a food cup, and a water bottle. The stimuli were white noise and a house light; the recorded responses were a press and release of the lever, head entries into the food cup, and licks on the tube of a water bottle; and the outcome was the delivery of a 45-mg pellet of food. The boxes were in sound-attenuating chambers. The feeders had a photocell circuit that produced up to five pulses to obtain a pellet in the food cup (with feedback about the time between request and delivery of a pellet). Two computers, using the Med-PC language, controlled Med Associates interface modules that monitored and controlled the equipment in the boxes.

Procedure.

Pretraining. The rats were initially trained to press the lever 30 times and receive a pellet of food following each response. The house light was turned on at the beginning of the session. During the first 30 min of this session, a pellet was also delivered every 60 s. The sessions ended with 30 lever presses or after 60 minutes, whichever occurred first. The house light was turned off at the end of the session. Additional sessions were given on subsequent days for rats that had not yet pressed the lever 30 times.

Training. The sessions of behavioral training of Groups 1 and 2 are shown in Table 2. The 24 rats of Group 1 (at four ages) were trained on a 128-s interval. The house light was turned on at the beginning of a session and off at the end of a session. A cycle consisted of (a) a white noise that began after an 8-s interval plus a random 24-s interval (exponentially distributed), (b) a food pellet that was delivered following the first lever response after 32 s from the onset of the white noise, (c) another food pellet that was delivered following the first lever response 128 s after the delivery of the previous food, and (d) the termination of the white-noise stimulus. Sessions began about 1:00 p.m.; they ended after 2 hr at the completion of the final cycle. There were 30 sessions. On all 30 sessions, the first lever response after 32 s from white-noise onset delivered a food pellet, and the first lever response 128 s after the delivery of these food pellets delivered another food pellet. (Dur-

Table 2
Behavioral Training of Group 1 and Group 2

	Behavioral training		
Group	Session	Interval (s)	Number of rats
Group 1	1–30	128	24
Group 2	1–40	64	12
Group 2	41–54	32	12
Group 2	55–68	64	12

ing the first 10 sessions, the temporal order of intervals was reversed on a random half of the intervals.)

The 12 rats of Group 2 (at four ages) were trained on intervals of 64 s, 32 s, and 64 s in three phases. The house light was turned on at the beginning of a session and off at the end of a session. The methods were similar to those used by Church, Meck, and Gibbon (1994). There were two types of cycles: food and nonfood cycles that were randomly intermixed. On food cycles, (a) a white noise was turned on after an 8-s interval plus a random 24 s (exponentially distributed), (b) a food pellet was delivered following the first lever response after a criterion interval, and (c) the white-noise stimulus terminated. This criterion interval was 64 s on Sessions 1 through 40, 32 s on Sessions 41 through 54, and 64 s on Sessions 55 through 68. Nonfood trials were also given. They were the same as the food trials except that no food was delivered and the white-noise stimulus remained on for a long fixed time (4 times the length of the fixed interval). On Sessions 1 through 10, the probability of a food trial was 0.5, and on the remaining Sessions 11 through 68, it was 0.25. The rats had two sessions each day that began at about 8:00 a.m. and about 8:00 p.m. After 2 hr, the session ended at the completion of the current cycle.

Biochemical Measurements

All measurement techniques have been previously published in step-by-step detail (Silverberg et al., 2010a, 2010b), with the exception of the BrdU labeling and the analysis of adult neurogenesis. The essential details are:

Aβ enzyme-linked immunosorbent assays (ELISA). Concentrations of Aβ40 and Aβ42, in cortical brain samples, were measured with a sandwich ELISA (Silverberg et al., 2010a). High-sensitivity ELISA kits (Wako Chemicals, Catalog #294–64701 and 292–64501, Richmond, VA) were chosen to reduce background noise and improve detection of Aβ40 (sensitivity: 0.049 pmol/L) and Aβ42 (sensitivity: 0.024 pmol/L). Both kits employ a two binding site sandwich ELISA designed to specifically detect Aβ40 and Aβ42. Brain samples were snap frozen in liquid N_2 and then ground into a powder on a bed of dry ice. Samples were extracted with both a 0.2% diethylamine (DEA)/50 mM NaCl solution and a 70% formic acid solution. Aβ40 and Aβ42 concentrations from both extracts were measured with the ELISA kits. Samples and standards were diluted with standard diluent, and added in duplicate to antibody-coated wells of a 96-well microtiter plate. Plates were incubated overnight at 4 °C. Following washing, samples were incubated for 2 hr (Aβ40) or 1 hr (Aβ42) at 4 °C with 100 μl of horseradish peroxidase (HR) conjugated antibody solution. Color was evolved by adding 100 μl of 3,3′,5,5′-tetramethylbenzidine solution to the wells. The reaction was terminated at 30 min with the stop solution. The plate was read on a Multiskan Plus spectrophotometer at 450 nm. Data were analyzed with DeltaSoft3 software (DeltaSoft, Hillsborough, NJ). Total protein was determined with a BCA Protein Assay kit (Pierce, Rockford, IL) with absorbance read at 562 nm. Total Aβ concentrations were expressed as pg/mg total protein.

LRP-1 and RAGE IHC. Brain samples were immersed in 4% paraformaldehyde in 0.4M Sorensen's phosphate buffer (SPB; pH 7.2) for 24 hr, and then cryoprotected in 30% sucrose with 0.1M SPB (pH 7.4; Hincherick, 1992). Specimens were snap frozen in liquid N_2, embedded in OCT compound (Sakura Finetek USA, Inc., Torrance, CA), and cryosectioned at 25 μm. After a quick rinse in Tris-buffered saline (TBS), the sections were quenched with 10% H_2O_2 for 10 min to eliminate endogenous peroxidase activity. This was followed by overnight blocking with 5% normal serum (Vector Laboratories, Burlingame, CA) at 4 °C. After blocking, sections were incubated overnight at 4 °C with the appropriate primary antibody: rabbit polyclonal LRP-1 (Orbigen, Catalog #PAB-10774, San Diego, CA; 1:75) or goat polyclonal RAGE (Affinity Bioreagents, Catalog #PA1–075, Golden, CO; 1:400). After washing sections in TBS, a secondary antibody (Vector Laboratories, Burlingame, CA; 1:500) is applied for 30 min at 20 °C. For LRP-1, a goat anti-rabbit IgG was used; and for RAGE, a rabbit anti-goat IgG was used. The ABC detection system (Vectastain Elite ABC Rabbit or Goat Peroxidase system; Vector Laboratories) was utilized. Sections were developed using 3,3-diaminobenzidine (DAB) as the chromogen, and then coverslipped/sealed with Cytoseal (Stevens Scientific, Riverdale, NJ), a xylene-based mounting medium. Positive control tissue (rat lung and liver) was run along with primary antibody omission controls.

Image analysis. Gray-scale images were obtained with an Olympus BH2-RFCA microscope (Olympus America, Inc., Mellville, NY) using a 40x objective. Images were acquired with a CoolSNAP compare camera (Roper Scientific, Tucson, AZ). For quantitative LRP-1 and RAGE expression (immunostaining surface area analysis), at least eight random fields were analyzed per specimen to establish the Aβ transporters in capillary endothelia. Cross-sections of cerebral microvessels (50 to 250 μm in diameter) were obtained from eight random field images acquired per specimen for analyses. Image processing was performed with ImageJ (v. 1.43, NIH, Bethesda, MD) along with previously reported analytical methods (Miller et al., 2008). For surface area calculations, all images were thresholded by the same observer at a single sitting to minimize the error associated with this analysis mode.

BrdU staining and neural stem cell proliferation analysis. For cell proliferation analysis, the F344/BN rats were injected with BrdU (Sigma-Aldrich, St. Louis, MO), 100 mg/kg ip, 1 hr prior to being euthanized by ip pentobarbital (125 mg/kg). BrdU is structurally classified as a halopyrimidine. More specifically, it is an analog of thymidine that incorporates into the DNA of actively dividing cells during the S phase of the cell cycle (Freese, O'Rourke, Judy, & O'Connor, 1994). Immediately after sacrifice, the brains were placed into 4% paraformaldehyde. Brains were then processed and embedded in paraffin, and sectioned at a thickness of 10 μm. After deparaffinization and rehydration, tissue sections were treated with hot (85 °C) 10 mM citrate buffer, pH 6, for 15 min. Sections were washed with distilled water and quenched with a peroxidase-blocking reagent (Dako, Carpinteria,

CA) for 10 min at room temperature to eliminate endogenous peroxidase activity. DNA was denatured by incubating sections in 2N HCl for 30 min at 37 °C; the acid was then neutralized by immersing sections in a 0.1M borate buffer for 10 min. After washing in 0.05M Tris-buffered saline with 0.05% Tween-20 (TBST), pH 7.6, sections were incubated overnight at 4 °C with a mouse monoclonal primary antibody directed against BrdU (Calbiochem, La Jolla, CA; Catalog # NA61, diluted 1:100). After washing the sections in TBST, an HRP-labeled polymer conjugated with secondary antibodies (anti-mouse; Dako, Catalog # K4000) was applied for 30 min at room temperature, in accordance with the EnVision + System for IHC staining. The tissue sections were washed in TBST and then stained using DAB (Dako) as the chromogen. Sections were dehydrated through a series of graded alcohols back to xylene, and then coverslipped and sealed using Cytoseal XYL (Richard-Allan Scientific, Kalamazoo, MI), a xylene-based mounting medium. Sixteen-bit gray-scale images were acquired with a Nikon E800 microscope (Nikon Inc., Melville, NY) using a 40x PlanApo objective. Camera settings were based on the darkest slide, and the camera's built-in green filter was used to increase image contrast (Diagnostic Instruments, Sterling Heights, MI). Image processing and analysis was performed using iVision image analysis software (BioVision Technologies, Inc., Exton, PA). Positive staining was defined through intensity thresholding, and the total number of positively stained cells per field was recorded.

Statistical Methods

Comparison of age groups on behavioral parameters. Twenty-four rats (4 ages $\times$ 6 rats = 24) were trained on a FI-128 s schedule of reinforcement for 30 days in a single phase. A second cohort of 12 rats (4 ages $\times$ 3 rats = 12) was trained in three phases: (a) 40 days FI-64 s, (b) 15 days FI-32 s, and (c) 15 days FI-64 s. The behavioral parameters were fit to the data from the last 10 days of each phase of training. In this way, the second cohort of rats had three sets of behavioral parameters, whereas the first cohort had only one set. Age groups for parameters were compared using separate generalized estimating equations (GEEs). The three replicates in each model from the second cohort were nested within rat. The omnibus model was a cell means model crossing age, phase, and interval trained. Age group means were constructed using linear estimates, which assigned 1/6 wt to each of the three replicated parameters (summing to [1/2]) from rats in the second cohort and [1/2] weight to the single parameter from the first cohort. In this way, the nested averages of rats from the second cohort were assigned equal weight to the single observations of rats from the first cohort (equally weighting rats). Six pairwise comparisons between these effects, as well as a single linear trend, were made by creating orthogonal contrasts from these weighted linear estimates. Alpha was maintained at 0.05 across the six pairwise comparisons between age groups using a Shaffer (1986) step-down Bonferroni adjustment to individual comparisons. Classical sandwich estimation was used to adjust for model misspecification in covariance parameters. The speed (the "A" parameter) was log-normal distributed, and thus means and confidence intervals from the lognormal GEE represented geometric means, once back-translated. Mu and sigma parameters were Gaussian.

Comparison of age groups on biochemical parameters. The analyses of biochemical parameters were analogous to those of the behavioral parameters, but did not require nesting or the creation of weighted estimates. A random effect was added to adjust for any overall change in intercept associated with the two cohorts.

Relationships among behavioral and biochemical parameters. Generalized linear models or, in the case of analyses involving behavioral parameters, GEEs were used to model the relationships between pairs of parameters; GEEs were implemented by accounting for nesting of multiple observations within rat as having correlated error. Again, classical sandwich estimation was used to adjust for model misspecification and distributions were selected based on inspection of model residual diagnostics.

Transition times. The transition times were calculated for a subset of three animals per age group that were trained on three sequential phases of fixed interval schedules of reinforcement to test for speed of learning new intervals (FI64 $\rightarrow$ FI32 $\rightarrow$ FI64). Attrition reduced the number of 30-month-old rats, and so only the 3-, 12-, and 20-month-old rats were analyzed. A seven-parameter nonlinear model was fit to the 40 session-by-session mean times of transition of each of the remaining rats. The model was composed of three exponential decay models fit to the three phases of training in sequence. The first phase contained parameters for a starting transition time, an asymptotic transition time, and the exponential rate of decay toward asymptote. The decay model for Phase 2 used the asymptotic transition time parameter from the previous phase as the starting parameter, and had its own exponential rate of decay and new asymptotic level. The third followed the same pattern, using the Phase 2 asymptote as its starting parameter, and had its own exponential rate of decay and asymptote. One model was fit to each rat, and the seven parameters used in statistical analysis. The exponential rates were converted to their percent remaining change, and all were analyzed in a general linear model comparing the three age groups allowing for correlated residuals within rat. Any model misspecification was compensated for using classical sandwich estimation. Comparisons between groups was not carried out on the "Start" parameter; however, three pairwise comparisons were carried out between the three age groups for each of the remaining parameters, with alpha maintained across all 18 pairwise comparisons using the Holm test.

Results

Behavioral Results

Speed, accuracy, and precision of performance. The primary data were the records of the times at which each stimulus (light or noise), reinforcer (food delivery), and response (lever press) occurred. Figure 1 shows how the data were analyzed. Panel a and Panel c are raster plots with dots that show the times of responses from onset of the white-noise stimulus for a 3-month rat (Panel a) and a 30-month rat (Panel c). The horizontal axis shows the time in seconds since the cycle began as a proportion of the 64-s interval. The vertical axis shows successive cycles on Sessions 21 through 30. Three features of these raster plots are (a) the relatively few responses early in the cycle and the higher response rate at the end of a cycle, (b) the time at which the response rate changed from low to high, and (c) the greater

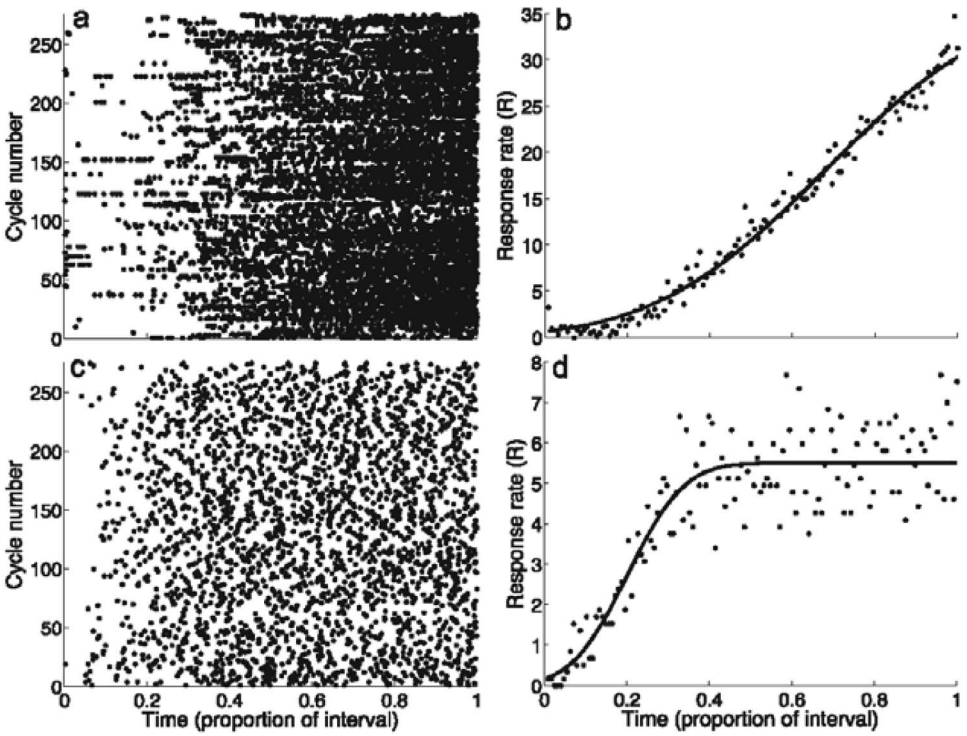

Figure 1. Measurement of behavioral parameters. The top panels (a and b) are data from a 3-month rat, and the bottom panels (c and d) are data from a 30-month rat. The left panels (a and c) show raster plots of the times of lever presses of two rats as a function of time since stimulus onset (in proportion of the interval) on all cycles (food to food intervals) of a single session. The right panels (b and d) show the mean response rate as a function of time since stimulus onset (in proportion of the interval) averaged over all cycles of the final five sessions of the 64-s condition.

density of the responses of the young rat (Panel a) than the old rat (Panel c), which indicates that the young rat was pressing the lever more rapidly than the old rat.

These raster plots are summarized by gradients shown in Panel b and Panel d. They show the mean response rate as a function of the proportion of time since a cycle began. The line is the best-fitting cumulative normal distribution. Three features of these cumulative normal functions are (a) the 30-month (Panel d) rat responded more slowly than the 3-month rat (Panel b)—note the response rates on the vertical axis; (b) the 30-month rat achieved its maximal response earlier in the interval than the 3-month rat; and (c) the 30-month rat increased its response rate more rapidly than the 3-month rat. These results were characteristic of most rats.

For quantitative analysis, these primary data were transformed into summary statistics. Sessions of these two rats are shown by the points in the right panels. These are the responses per minute in 1-s intervals, plotted as the proportion of the interval. (The fits are based on the proportion of the interval between 0 and 1.) The S-shaped functions (solid lines) are the least-squares fits of the data to Equation 1:

$$Y = A * \phi(\mu, \sigma) + r \quad (1)$$

This is a cumulative normal distribution with a mean (μ), a standard deviation (σ), and a transformation with a minimum response rate (r), and a multiplier (A). These values were obtained for each of the 36 rats.

The behavioral measures were the speed ($\log_{10}$A), accuracy (μ), and precision ($1-\sigma$) of responding. Speed increases as the asymptote increases. Accuracy increases as the mean proportion of the interval approaches the time of reinforcement (1.0). Note that precision ($1-\sigma$) increases as the standard deviation decreases. The three parameters (speed, accuracy, and precision of responding) are independent, that is, the selection of the value of any two of the parameters *does not limit the range of the third parameter*.

***Behavioral parameters as* a function of age.** Behavioral aging was characterized by a decrease in speed and accuracy, and an increase in precision. These results are shown in Figure 2.

The speed parameter (Panel a) was higher in younger rats than in older rats. This was tested both as a priori pairwise comparisons between age groups and as a trend. Pairwise comparisons resulted in statistically significant differences between each of the two youngest age groups (3- and 12-months-old) and each of the two oldest age groups (20- and 30-months-old), but not statistically significant difference between the 3- and 12-month groups or between the 20- and 30-month old groups. This suggests the possibility of a particularly rapid age-related change of speed between 12 and 20 months of age. More specifically, the speed parameters of 3-month-old rats were significantly higher than those of 20-month (adjusted [adj.] $p = .003$) and 30-month rats (adj. $p = .031$), but not 12-month rats (adj. $p = .934$); and the speed parameters of 12-month rats were significantly higher than those of 20-month rats (adj. $p < .001$) and 30-month rats

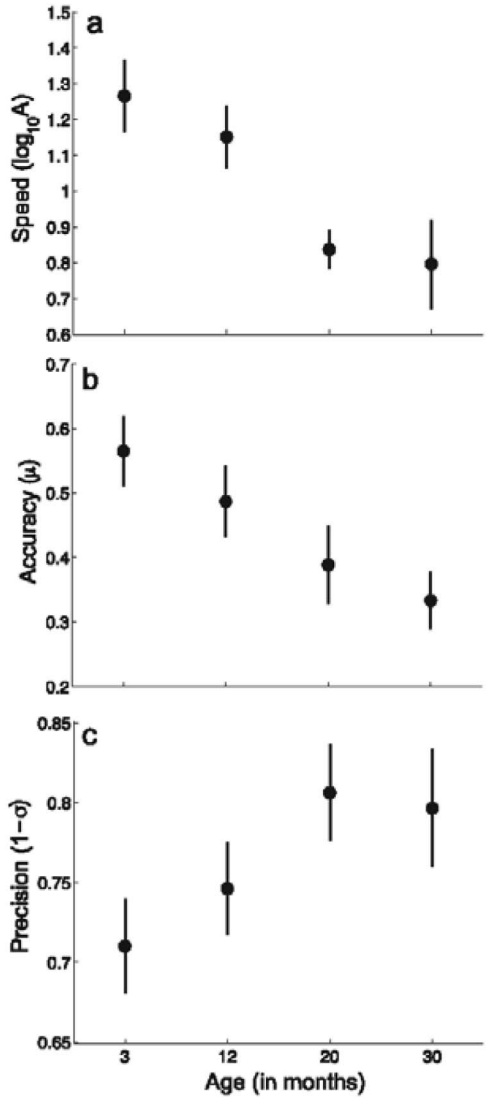

Figure 2. Behavioral aging. The top panel (a) is response speed, the middle panel (b) is response accuracy, and the bottom panel (c) is response precision. The basis for these measures are shown in Figure 1 and defined by Equation 1 in the text.

(adj. $p = .002$), which did not differ from one another (adj. $p = .934$). The test for a trend across the groups was also statistically significant (adj. $p = .004$). This is not inconsistent with the pattern of pairwise differences, and it does not rule out the possibility that there is both a decreasing trend and a more rapid change between 12 and 20 months.

A similar pattern of effects was observed regarding the accuracy parameter (Panel b), although the pairwise differences were not as pronounced. Specifically, 3-month rats again did not differ from 12-month rats (adj. $p = .387$), and had higher accuracy parameters than 20-month rats (adj. $p = .023$) and 30-month rats (adj. $p = .023$); and again, 20-month rats and 30-month rats did not differ significantly (adj. $p = .309$). However, 12-month rats did not differ significantly from 20-month (adj. $p = .054$) or 30-month rats (adj. $p = .054$). The test for a trend across age groups was again significant ($p = .003$). This does not rule out the possibility that there is both a trend and a more rapid transition blurred by random error.

The test for trend in the precision parameter (Panel c) was again significant (adj. $p = .023$), but none of the pairwise differences between age groups were statistically significant. Thus, the speed, accuracy, and precision were related to age, and there were changes in the speed and accuracy of rats between 12 and 20 months of age. The lack of pairwise differences for the precision measure suggests that it was less robust than the others.

Relationships among behavioral measures. The three measures of behavioral aging shown in Figure 3 (speed, accuracy, and precision) were all statistically significantly related to one another (accuracy as a function of precision, $p < .001$; accuracy as a function of speed, $p < .001$; precision as a function of speed, $p < .001$). Speed and accuracy were positively related; precision was negatively related to both speed and accuracy.

Response gradients in the peak procedure. Twelve rats had both food and nonfood cycles. The top panel of Figure 4 shows the mean responses per minute on Sessions 30 through 40 as a function of time relative to expected food (i.e., the time since stimulus onset divided by 64 s, which was the time of the food cycles). At all ages, the response rate increased to a maximum near the time that food appeared, and then it decreased. The primary differences were that the response rate of the older rats was lower than the younger rats, and that there was a large difference between 12- and 20-month rats.

The speed parameter was higher for 3- and 12-month rats than for 20-month rats (vs. 3, $p = .002$, adj. $p = 0.006$; vs. 12, $p < .001$, adj. $p < .001$) and 30-month rats before, but not after, alpha adjustment (vs. 3, $p = .022$, adj. $p = .051$; vs. 12, $p = .016$, adj. $p = .051$). Speed was not statistically significantly different between 3- and 12-month old rats ($p = .951$, adj. $p = .951$) or between 20- and 3-month rats ($p = .308$, adj. $p = .616$).

The accuracy parameters of the 12-month rats were closer to 1.0 (i.e., more accurate) than other three ages (vs. 3, $p = .021$, adj. $p = .042$; vs. 20, $p < .001$, adj. $p = 002$; vs. 30, $p = .009$, adj. $p = .027$). Additionally, the 3-month rats were more accurate than the 20-month ($p = .001$, adj. $p = .004$) and 30-month ($p = .022$, adj. $p = .042$) rats, which did not differ from each other ($p = .343$, adj. $p = .343$).

Precision did not differ between 3- and 12-month rats ($p = .329$, adj. $p = .357$), which had higher precision than 20-month rats (vs. 3, $p = .003$, adj. $p = .012$; vs. 12, $p = .002$ adj. $p = .012$). The 30-month rats were highly variable and did not differ significantly from any of the other age groups (vs. 3, $p = .068$, adj. $p = .188$; vs. 12, $p = .063$, adj. $p = .188$; vs. 20, $p = .179$, adj. $p = .357$).

The same data are replotted in the bottom panel of Figure 4, with the response rate plotted as relative response rate (response rate divided by maximum response rate) rather than as absolute response rate (responses per min). On this scale, the behavior of the rats is similar from the onset of the stimulus until the food had been available, but the relative response rate of the old rats (20 and 30 months) was higher than the relative response rate of the young rats (3 and 12 months).

Transition time as a function of days of training of rats of different ages. To assess the speed of learning, the transition time was identified for each food and nonfood cycle of the 12 rats on all 68 sessions. Typically, a raster plot of a cycle has few

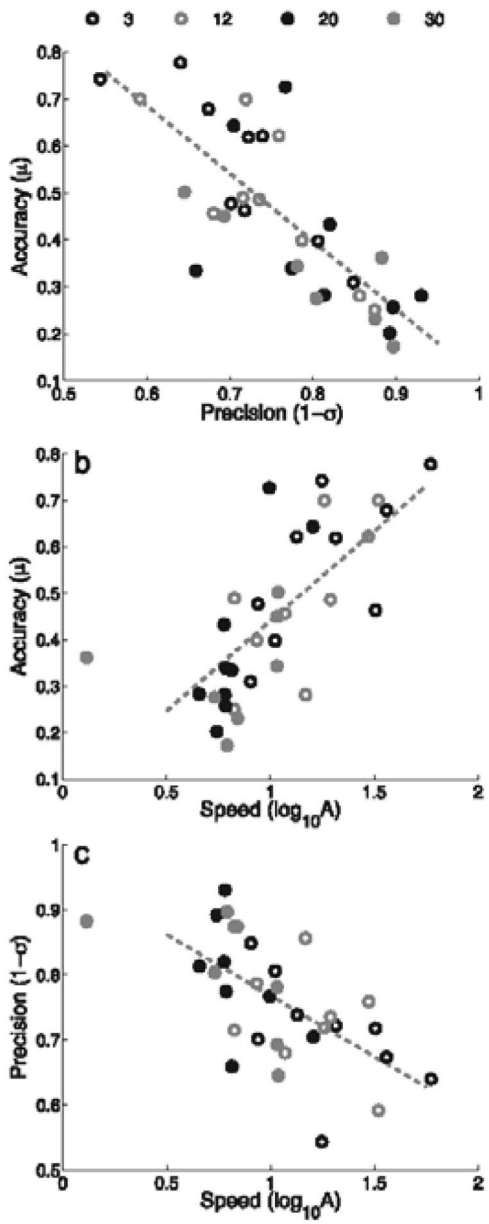

Figure 3. Relationships between behavioral measures. The relationships between response speed, response accuracy, and response precision are shown in the three panels.

responses at the beginning and many responses at the end. Equation 2 was used to identify a single transition from the low response rate to the high response rate. This transition time was used as a measure of accuracy. On each cycle, an exhaustive search was made for the time t_i that maximized the change in the response rate:

$$\text{Max } t_i = d_1(r - r_1) + d_2(r_2 - r) \quad (2)$$

where d_1 and d_2 are the durations before and after t_i, r_1 and r_2 are the response rates before and after t_i, and r is the response rate during the entire cycle.

Figure 5 shows the mean transition times for each day of training for each of the rats in each of the four age groups. (The 30-month group was not included in the statistical analysis because one of the three rats died, and one was an outlier.) There was gradual initial learning of the 64-s interval, but a rapid learning of the subsequent 32-s interval, and the return to the 64-s interval. The pairwise comparisons of the three age groups (3, 12, and 20 months) on the seven parameters only identified one of the comparisons as significant. This experiment did not provide evidence that there is an age-related difference in the speed of original learning or the speed of transition from one interval (such as 64 s) to another (such as 32 s).

Biochemical Results

Biochemical aging. Biochemical aging was characterized by an increase in the level of Aβ40, Aβ42, and RAGE expression, and a decrease in LRP-1, as shown in Figure 6. The statistical analysis of the four age groups tested in this experiment (black

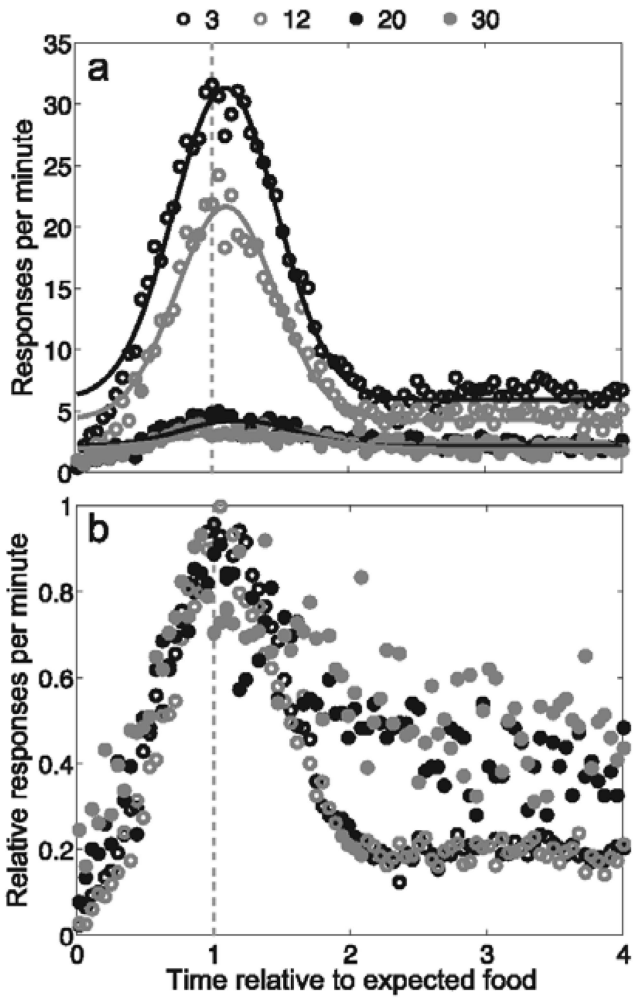

Figure 4. Response gradients in the peak procedure. The top panel (a) is response rate as a function of relative time to expected food. The bottom panel (b) is relative response rate as a function of relative time to expected food.

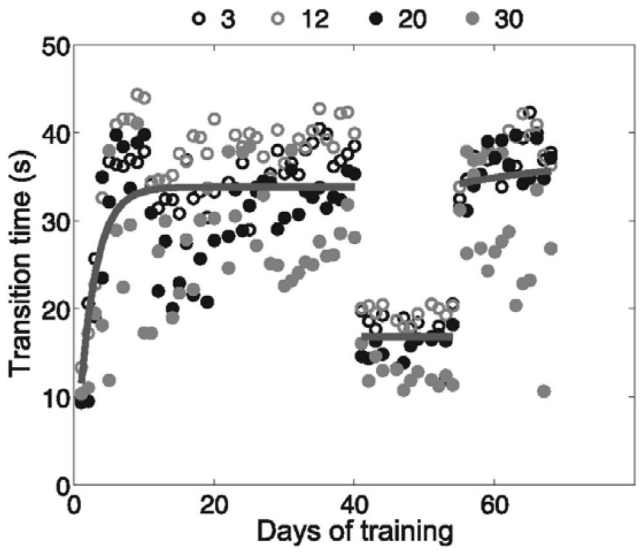

Figure 5. Transition time in seconds as a function of days of training for rats at 3, 12, 20, and 30 months. Food was available for the first response after stimulus onset on Days 1 to 40 at 64 s, on Days 41 to 54 at 32 s, and on Days 55 to 68 at 64 s.

symbols) is described in this section. Previously published research (gray symbols) shows similar results from more age groups (Silverberg et al., 2010a, 2010b).

Aβ40 was lower in 3-month rats than any of the other three age groups (vs. 12, adj. $p = .002$; vs. 20, adj. $p < .001$; vs. 30, adj. $p < .001$). None of the other three age groups differed significantly (12 vs. 20, adj. $p = .217$; 12 vs. 30, adj. $p = .217$; 20 vs. 30, adj. $p = .843$). A test for a trend was statistically significant ($p < .001$).

Aβ42 showed more clear progressive differences, with 3-month rats having significantly lower Aβ42 than the other three age groups (vs. 12, adj. $p = .009$; vs. 20, adj. $p < .001$; vs. 30, adj. $p < .001$); 12-month rats having significantly lower Aβ42 than 20-month (adj. $p = .0216$) and 30-month rats (adj. $p = .0041$); and no statistically significant difference between 20- and 30-month rats (adj. $p = .1184$). The trend for Aβ42 was also statistically significant ($p < .001$).

The inverse pattern of differences was observed in LRP-1, with 3-month rats significantly higher LRP-1 levels than the other three age groups (adj. $p = .0476$ for all comparisons), and no statistically significant difference among 12, 20, and 30 month old rats (adj. $p = .518$ for all comparisons), along with a statistically significant trend ($p = .0064$).

For RAGE, 3- and 12-month rats did not differ significantly (adj. $p = .284$), both differed from 20-month (adj. $p = .016$, and adj. $p = .033$, respectively) and 30-month rat (adj. $p < .001$, and adj. $p = .006$, respectively), and 20- and 30-month rats did not differ significantly (adj. $p = .813$).

Representative photomicrographs of an LRP-1 and RAGE-stained vessel at 3 and 30 months are shown in Figure 7. The LRP-1 efflux transporter decreased with age, and the RAGE influx transporter increased with age.

Cell proliferation with aging. BrdU analysis showed a significant decrease in neurogenesis as measured by BrdU labeled cell counts (see Figure 8). In the SVZ (Panel b), the mean (± *SD*) value for BrdU-immunopositive SVZ cell counts in 3-month-old rats was 628.8 ± 33.95 cells ($n = 5$); at 12 months, it was 673.4 ± 30.01 cells ($n = 5$); at 20 months, it was 364 ± 15.41 cells ($n = 5$); and at 30 months, it was 324.8 ± 42.34 cells ($n = 5$). Cell proliferation in the SVZ was greater for the young rats (3- and 12-month rats) than for the old rats (20- and 30-month) for all comparisons (adj. $p < .001$). Differences between 3- and 12-month rats and the 20- and 30-month old rats approached significance, but did not differ significantly (adj. $p = .051$).

In the DG, the mean (± *SD*) value for BrdU-immunopositive cell counts in 3-month-old rats was 514.8 ± 81.59 cells ($n = 5$); at 12 months, it was 496.2 ± 86.64 cells ($n = 5$); at 20 months, it was 445.8 ± 96.48 cells ($n = 5$); and at 30 months, it was 304.4 ± 169.53 cells ($n = 5$). Cell proliferation in the DG was more gradual as a function of age, with a statistically significant downward trend with age ($p = .010$), but no statistically significant differences between pairs of ages (adj. ps $> .07$).

The photomicrographs (see Figure 9) show the distribution of BrdU immunoreactivity in the SVZ and the DG of the hippocampus in single rats at the four ages (3, 12, 20, and 30 months).

In the SVZ (Panels A through D), there was a substantial reduction in the number of BrdU-immunopositive nuclei as a function of aging, especially between 12 and 20 months of age (Panels B and C).

In the DG of the hippocampus, there was also a substantial decrease in BrdU-immunopositive cell count between the 3- and 30-month rats (Panels E and H).

Relationships among biochemical measures. The relationships between Aβ40, Aβ42, RAGE, and LRP-1 are shown in the six panels. All biochemical measures were statistically significantly related to one another ($p < .05$ for each combination).

Table 3 provides the relationship of four biochemical measures (Aβ40, Aβ42, RAGE, and LRP-1) with three behavioral measures (speed, accuracy, and precision). It provides the correlations (*r*s) and the probability values (*p*s). There were no statistically significant relationships of any of the behavioral measures with LRP-1, which likely acts upon behavior only through its effect on amyloid accumulation The other three biochemical measures were significantly related to the three biochemical measures. Aβ40, Aβ42, and RAGE were negatively related to speed and accuracy, and positively related to precision.

Discussion

The goals of this article were to describe age-related biochemical changes and age-related behavioral changes, and describe the relationship between the biochemical and behavioral changes. The biochemical changes were (a) the expression of the major BBB Aβ transport receptor proteins, LRP-1, and RAGE, also known as AGER; (b) the increase in Aβ concentration in the brain tissue; and (c) the alterations in neural stem proliferation. The behavioral changes focused on the speed, accuracy, and precision of behavioral responses, and the speed and pattern of learning.

Chronological age is an important risk factor for many diseases, and for death. Aging is the single most important risk factor for the genesis of AD (National Institute of Aging, 2002). Advancing age is characterized by both age-related biochemical

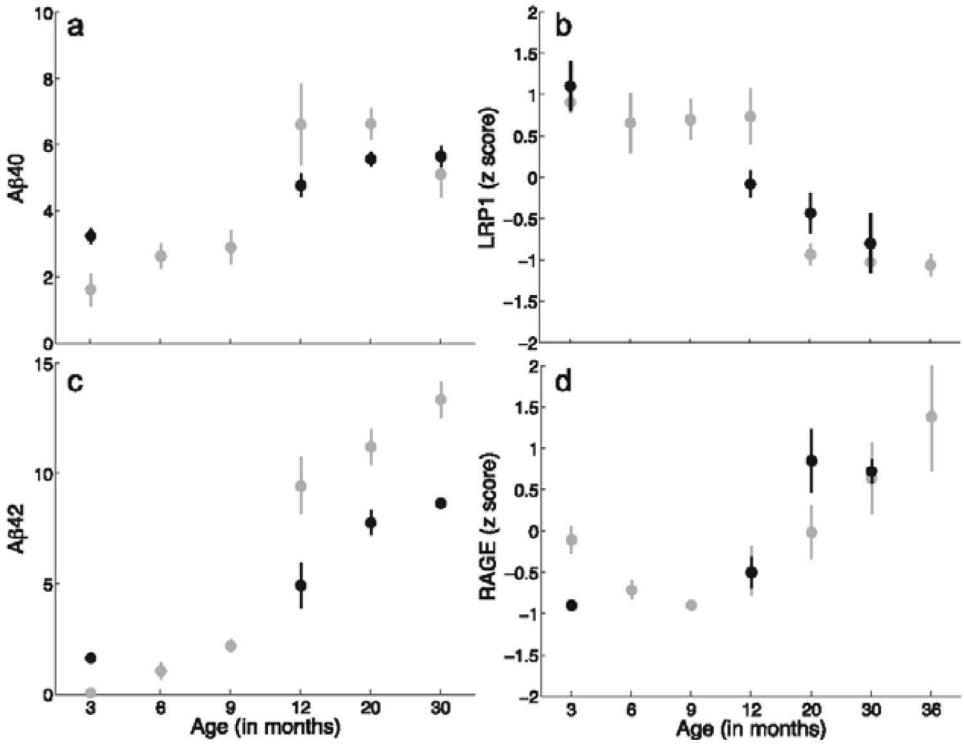

Figure 6. Biochemical aging. Aβ40 (Panel a) and Aβ42 concentrations (Panel c), and endothelial expression of the amyloid efflux transporter LRP-1 (Panel b) and the endothelial expression of the amyloid influx transporter RAGE (Panel d). The black markers are from the present experiment, and the gray markers refer to data from Silverberg et al. (2010a, 2010b).

changes and age-related behavioral changes. Both of these measures provide estimations of chronological age, as shown in Figures 2 and 6. But the main function they serve is to provide a better understanding of the mechanisms responsible for age-related changes.

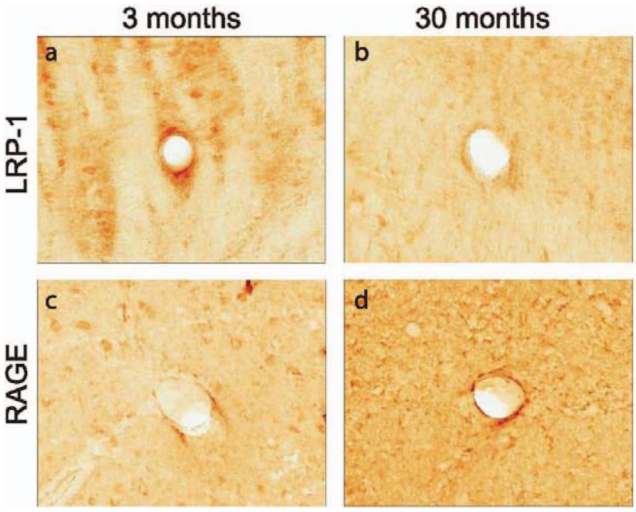

Figure 7. Representative photomicrographs of an LRP-1 and RAGE-stained vessel at 3 and 30 months: 3-month LRP-1 (Panel a), 30-month LRP-1 (Panel c), 3-month RAGE (Panel b), and 30-month RAGE (Panel d).

The temporal profile of age-related Aβ accumulation in the F344/BN rat is one of progressively altered transport of this potentially toxic peptide out of the brain (Chiu et al., 2012; Pascale et al., 2011; Silverberg et al., 2010a, 2010b). The most important conduit for Aβ removal is by active transport across the BBB (Zlokovic, Yamada, Holtzman, Ghiso, & Frangione, 2000), although there is some in situ degradation and some transport by the bulk flow of CSF and across the choroid plexus epithellium (Chiu et al., 2012; Iwata et al., 2000; Pascale et al., 2011). At the BBB in this study, there was a decrease in efflux transporter expression and an increase in influx transporter expression, leading to an increasing concentration of Aβ in brain parenchyma. We found a significant early and progressive decrease in LRP-1 expression and a significant and progressive increase in RAGE expression. The efflux transporter P-gp also decreases significantly but not until late in aging in the F344/BN rat (Silverberg et al., 2010b). As these BBB transporters are general scavengers and transport a wide variety of unrelated solutes, other potential toxins may also be retrained in the brain with aging, not just Aβ (Fromm, 2004; Herz & Strickland, 2001; Schmidt et al., 1994).

It is generally accepted that Aβ accumulation in the human brain is neurotoxic and likely begins the "amyloid cascade," the hypothesis that accumulation of Aβ within the brain (particularly

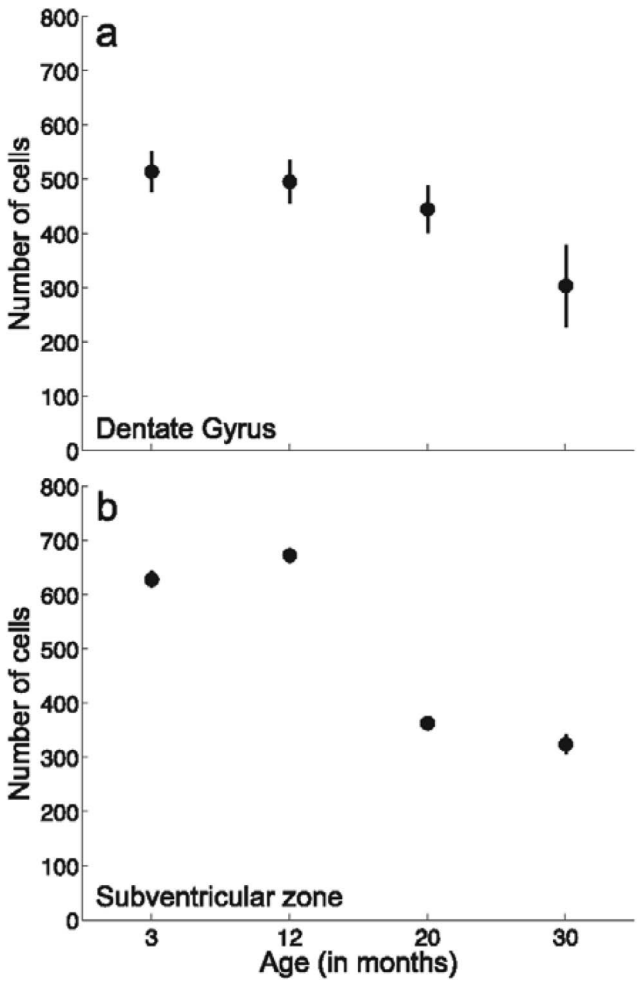

Figure 8. Neurogenesis as a function of age. The BrdU-labeled neural stem cell counts are shown for the dentate gyrus (Panel a) and the subventricular zone (Panel b) at the four ages.

Aβ42) triggers the development of AD pathology and underlies cognitive decline (Hardy & Selkoe, 2002; Querfurth & LaFerla, 2010). The adverse effects of human Aβ oligomers and intermediate forms of Aβ on neuronal viability, synaptic plasticity, and synaptic function have now been repeatedly demonstrated (Querfurth & LaFerla, 2010). Although Aβ monomers support neuronal survival (Giuffrida et al., 2009), the formation of Aβ oligomers and intermediates that occur when Aβ accumulates (Esler, Stimson, Ghilardi, et al., 1996), significantly impacts cognition. It is well known that rodent Aβ differs from human Aβ and is less toxic (Esler, Stimson, Jennings, et al., 1996). That difference makes it impossible for rodent Aβ to form protofibrils, fibrillary Aβ β-sheets, and amyloid plaques as human Aβ can do. However, rodent Aβ can form oligomers in a concentration dependent manner (Esler, Stimson, Jennings, et al., 1996).ates that occur when Aβ accumulates (Esler, Stimson, Ghilardi, et al., 1996), significantly impacts cognition Nanomolar concentrations of human oligomeric Aβ are sufficient to induce neuronal death in rodent organotypic hippocampal slice cultures in the absence of protofibrils or fibrillar Aβ, and will inhibit the long-term potentiation that underlies memory (Lambert et al., 1998; Selkoe, 2002; Walsh et al., 2002; Witton et al., 2010). Other studies have shown that high levels of oligomeric Aβ cause synaptic transmission deficiency in rodents by impairing the reactivity of synaptophysin, the formation of toxic protofibrils, and the impaired regulation of synaptic actin (Mucke et al., 2000; O'Nuallain, et al., 2010; Penzes & VanLeeuwen, 2011). In addition, increasing Aβ concentrations lower neurogenesis from pluripotent stem cells by suppressing cell differentiation (Shruster et al., 2011; Wicklund et al., 2010). The present study shows that age-related Aβ accumulation is associated with significant behavioral changes and inhibition of neurogenesis. The aging F344/BN rat could be a model for the study of the aging human brain.

Monoclonal antibodies directed against single-stranded DNA containing BrdU can detect its immunoreactivity by IHC (Gratzner, 1982). Compared with alternatives like 3H-thymidine autoradiography (Angevine, 1965; Sidman, 1970), the relative ease of utilizing BrdU has greatly contributed to it becoming the most widely used method for studying adult neurogenesis in situ (Kee, Sivalingam, Boonstra, & Wojtowicz, 2002; Taupin, 2007). The BrdU analysis from the F344/BN rats in this study shows a profound effect of aging on neural stem cell counts, particularly in the SVZ.

A limitation encountered was that we were unable to run IHC for both the BBB Aβ transporters (LRP-1 and RAGE) and BrdU on the same set of rats due to the very different tissue preparations required for both types of antibodies to yield optimal staining. Our group has previously demonstrated that the ideal signal-to-noise ratio for both LRP-1 and RAGE immunoreactivity is obtained when using free-floating thick (20 to 50 μm) fixed-frozen tissue sections throughout the entire protocol (Miller et al., 2008; Silverberg et al., 2010a; Silverberg et al., 2010b). Unfortunately, sections prepared using this method are unable to withstand the DNA denaturing steps required for binding of the BrdU-specific antibody to its epitope. To corroborate our former findings on age-related transporter expression, and to have data that could be correlated directly with behavioral measures, we opted to use the brains obtained from the behaviorally tested rats for the transporter IHC rather than BrdU staining.

Given that neural stem cell proliferation is critical to maintaining hippocampal and cortical neuronal networks that underlie memory and cognition (Artegiani & Calegari, 2012; Deng, Aimone, & Gage, 2010; Ming & Song, 2011), we obtained a second set of F344/BN rats to investigate BrdU expression along a continuum of the four age groups (3, 12, 20, and 30 months). Neural stem cells in the rat brain are generally confined to two forebrain areas: the subgranular zone/DG of the hippocampus and the SVZ. Growing evidence suggests that although these neural stem cells may be small in number, they contribute to the generation of neurons, via intermediates, that are continuously incorporated into the brain circuitry throughout a life span (Kempermann, 2008; Marín -Burgin & Schinder, 2012). As such, we performed software-assisted cell counting of BrdU-immunopositive nuclei in the DG and SVZ in this second set of rats across the four age groups. We found evidence of an age effect in both anatomical brain regions: A significant decrease in cell count was most notable for the DG when comparing 3- versus 30-month rats, whereas an earlier

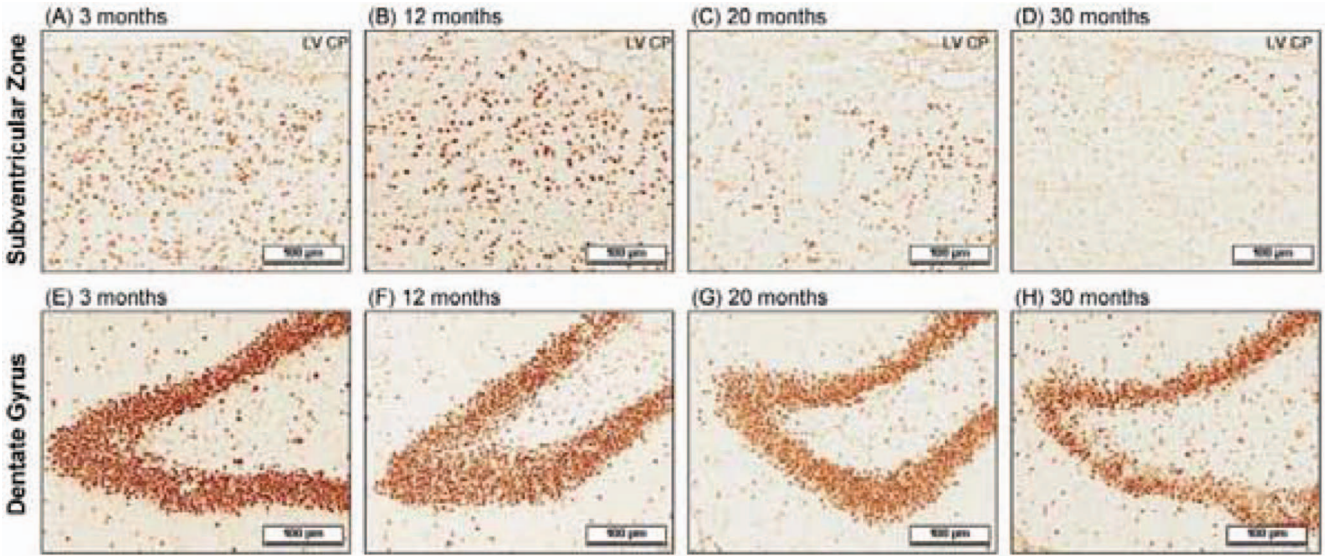

Figure 9. Representative bright-field photomicrographs (100x magnification) demonstrate the distribution of BrdU immunoreactivity in the F344/BN rat subventricular zone (Panels A to D) and dentate gyrus (E to H) at the four ages.

drop-off (between 12 and 20 months) was witnessed for the SVZ. The decrease in BrdU-positive SVZ nuclei notably follows the sharpest rise in the temporal progression of Aβ accumulation in the F344/BN rat (Silverberg et al., 2010a) and the onset of behavioral decline.

It is also now generally accepted that the pathology of AD begins long before the onset of actual cognitive impairment (De Meyer et al., 2010), with changes that may begin as early as early middle age (Lu et al., 2004; Yankner, Lu, & Loerch, 2008). Our F344/BN rat model shows that the expression of the Aβ efflux transporter LRP-1 decreases significantly with age, beginning at about six months, whereas RAGE, the Aβ influx transporter, expression increases with age, beginning between 9 and 12 months. Aβ accumulation increases between 9 and 12 months as well, and between 12 and 20 months, there is a significant reduction in neurogenesis and behavioral measures on our test paradigm.

Age-related biochemical changes provide a basis for predicting the effect of experimental procedures at different ages.

Table 3
Relationships Between Biochemical and Behavioral Measures

	Behavioral					
	Speed		Accuracy		Precision	
Biochemical	*r*	*p*	*r*	*p*	*r*	*p*
Aβ40	−655*	<.001	−.485*	.007	+.461*	.010
Aβ42	−583*	<.001	−.508*	.004	+.369*	.048
RAGE	−550*	.042	−.554*	.040	+.554*	.040
LRP-1	+307	.285	+.231	.426	−.058	.844

Note. Aβ40 and Aβ42 = amyloid-beta peptides; RAGE = receptor for advanced glycation end products; LRP-1 = low-protein lipoprotein receptor-related protein.
* $p < .05$.

These predictions can also be made by computational models. In this article, a simple equation (Equation 1) was used to fit summary data (see Figure 1), and parameters of this equation were used to estimate the values of speed, accuracy, and precision. Although this is a curve-fitting approach, its strength is that it can be derived from a computational model of learning and performance (Guilhardi, Yi, & Church, 2007). The added strength of a computational model is its generality, that is, it can make predictions about all summary measures based upon the primary data (Guilhardi & Church, 2009).

Both the behavioral and biochemical accounts of age-related changes depend on the use of multiple measures. The high correlation of the behavioral measures with each other (see Figure 3) and the biochemical measures with each other (see Figure 10) indicate that the different measures are not independent. The high correlations between the biochemical and behavioral measures (see Table 3) indicate that the two types of measures are not independent. This suggests that behavioral measures may serve as surrogate markers of biochemical changes in the brain, for example, Aβ accumulation, neurogenesis, and other biochemical events.

Some of the behavioral and biochemical measures changed particularly rapidly between 12 and 20 months of age. The statistical analyses used pairwise comparisons, as well as a single linear trend, to identify these changes. The relatively abrupt changes between 12 and 20 months were particularly clear in the behavioral measure of response speed, the biochemical measures of the Aβ influx transporter RAGE, and the neurogenesis cell proliferation in the SVZ of the hippocampus. These changes between 12 and 20 months are substantially earlier than the median of the life span of the F344/BN rats, which is about 36 months (Turturro et al., 1999). These, possibly rapid, changes in amyloid accumulation and processing speed may provide opportunity to identify individuals who will

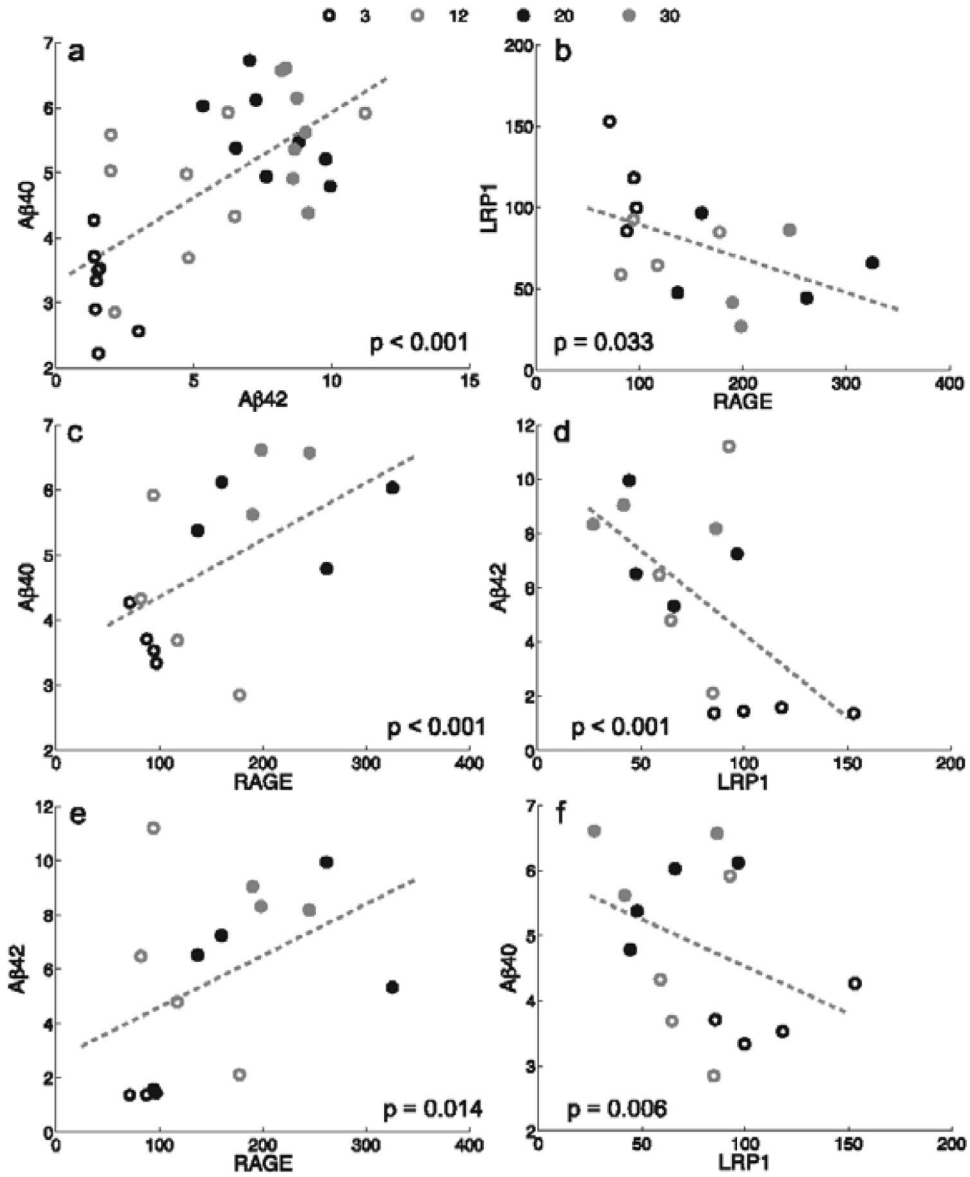

Figure 10. Relationships between biochemical measures Aβ40, Aβ42, RAGE, and LRP-1 are shown in the six panels.

benefit from therapeutic effort before the onset of irreversible AD pathology.

References

Angevine, J. B., Jr. (1965). Time of neuron origin in the hippocampal region. An autoradiographic study in the mouse. *Experimental Neurology, 11,* 1–70. doi:10.1016/0014-4886(65)90121-4

Artegiani, B., & Calegari, F. (2012). Age-related cognitive decline: Can neural stem cells help us? *Aging, 4,* 176–186.

Boonstra, R. (2005). Equipped for life: The adaptive role of the stress axis in male mammals. *Journal of Mammalogy, 86,* 236–247. doi:10.1644/BHE-001.1

Chiu, C., Miller, M. C., Caralopoulos, I. N., Worden, M. S., Brinker, T., Gordon, Z. N., . . . Silverberg, G. D. (2012). Temporal course of cerebrospinal fluid dynamics and amyloid accumulation in the aging rat brain from three to thirty months. *Fluids and Barriers of CNS, 9,* 1–8.

Church, R. M., Meck, W. H., & Gibbon, J. (1994). Application of scalar timing theory to individual trials. *Journal of Experimental Psychology: Animal Behavior Processes, 20,* 135–155. doi:10.1037/0097-7403.20.2.135

Curlik, D. M., II, & Shors, T. J. (2013). Training your brain: Do mental and physical (MAP) training enhance cognition through the process of neurogenesis in the hippocampus? *Neuropharmacology, 64,* 506–514. doi:10.1016/j.neuropharm.2012.07.027

De Meyer, G., Shapiro, F., Vanderstichele, H., Vanmechelen, E., Engelborghs, S., De Deyn, P. P., . . . Trojanowski, J. Q. (2010). Diagnosis-independent Alzheimer disease biomarker signature in cognitively normal elderly people. *Archives of Neurology, 67,* 949–956. doi:10.1001/archneurol.2010.179

Deng, W., Aimone, J. B., & Gage, F. H. (2010). New neurons and new memories: How does adult hippocampal neurogenesis affect learning and memory? *Nature Reviews. Neuroscience, 11,* 339–350. doi:10.1038/nrn2822

Eriksson, P. S., Perfilieva, E., Bjork-Eriksson, T., Alborn, A. M., Nordborg, C., Peterson, A., & Gage, F. H. (1998). Neurogenesis in the adult human hippocampus. *Nature Medicine, 4,* 1313–1317. doi:10.1038/3305

Esler, W. P., Stimson, E. R., Ghilardi, J. R., Vinters, H. V., Lee, J. P., Mantyh, P. W., & Maggio, J. E. (1996). In vitro growth of Alzheimer's disease beta-amyloid plaques displays first-order kinetics. *Biochemistry, 35,* 749–757. doi:10.1021/bi951685w

Esler, W. P., Stimson, E. R., Jennings, J. M., Ghilardi, J. R., Marityh, P. W., & Maggio, J. E. (1996). Zinc-induced aggregation of human and rat beta-amyloid peptides in vitro. *Journal of Neurochemistry, 66,* 723–732. doi:10.1046/j.1471-4159.1996.66020723.x

Fontana, L., & Klein, S. (2007). Aging, adiposity, and calorie restriction. *Journal of the American Medical Association, 297,* 986–994. doi:10.1001/jama.297.9.986

Freese, A., O'Rourke, D., Judy, K., & O'Connor, M. J. (1994). The application of 5-bromodeoxyuridine in the management of CNS tumors. *Journal of Neuro-Oncology, 20,* 81–95. doi:10.1007/BF01057964

Fromm, M. F. (2004). Importance of P-glycoprotein at blood-tissue barriers. *Trends in Pharmacological Sciences, 25,* 423–429. doi:10.1016/j.tips.2004.06.002

Gallagher, M., & Rapp, P. (1997). The use of animal models to study the effects of aging on cognition. *Annual Review of Psychology, 48,* 339–370. doi:10.1146/annurev.psych.48.1.339

Gallagher, M., Stocker, A., & Koh, M. T. (2011). Mindspan: Lessons from rat models of neurocognitive aging. *ILAR Journal, 52,* 32–40. doi:10.1093/ilar.52.1.32

Giuffrida, M. L., Caraci, F., Pignataro, B., Cataldo, S., De Bona, P., Bruno, V., . . . Copani, A. (2009). β-Amyloid monomers are neuroprotective. *The Journal of Neuroscience, 29,* 10582–10587. doi:10.1523/JNEUROSCI.1736-09.2009

Gould, E., Beylin, A., Tanapat, P., Reeves, A., & Shors, T. J. (1999). Learning enhances adult neurogenesis in the hippocampal formation. *Nature Neuroscience, 2,* 260–265. doi:10.1038/6365

Gratzner, H. G. (1982, October 29). Monoclonal antibody to 5-bromo- and 5-iododeoxyuridine: A new reagent for detection of DNA replication. *Science, 218,* 474–475. doi:10.1126/science.7123245

Guilhardi, P., & Church, R. M. (2009). The generality of empirical and theoretical explanations of behavior. *Behavioural Processes, 81,* 205–215. doi:10.1016/j.beproc.2009.01.013

Guilhardi, P., Yi, L., & Church, R. M. (2007). A modular theory of learning and performance. *Psychonomic Bulletin & Review, 14,* 543–559. doi:10.3758/BF03196805

Hardy, J., & Selkoe, D. J. (2002, July 19). The amyloid hypothesis of Alzheimer's disease: Progress and problems on the road to therapeutics. *Science, 297,* 353–356. doi:10.1126/science.1072994

Herz, J., & Strickland, D. K. (2001). LRP: A multifunctional scavenger and signaling receptor. *Journal of Clinical Investigation, 108,* 779–784. doi:10.1172/JCI200113992

Hincherick, F. R. (1992). Transmission electron microscopy. In E. B. Prophet, B. Mills, J. B. Arrington, & L. H. Sobin (Eds.), *Laboratory methods in histotechnology* (pp. 257–263). Washington, DC: American Registry of Pathology.

Iwata, N., Tsubuki, S., Takaki, Y., Watanabe, K., Sekiguchi, M., Hosoki, E., . . . Saido, T. (2000). Identification of the major Abeta 1-42-degrading catabolic pathways in brain parenchyma: Suppression leads to biochemical and pathological deposition. *Nature Medicine, 6,* 143–150. doi:10.1038/72237

Kee, N., Sivalingam, S., Boonstra, J. M., & Wojtowicz, J. M. (2002). The utility of Ki-67 and BrdU as proliferative markers of adult neurogenesis. *Journal of Neuroscience Methods, 115,* 97–105. doi:10.1016/S0165-0270(02)00007-9

Kempermann, G. (2008). The neurogenic reserve hypothesis: What is adult hippocampal neurogenesis good for? *Trends in Neurosciences, 31,* 163–169. doi:10.1016/j.tins.2008.01.002

Lambert, M. P., Barlow, A. K., Chromy, B. A., Edwards, C., Freed, R., Liosatos, M., . . . Klein, W. L. (1998). Diffusible, nonfibrillar ligands derived from $A\beta_1$–42 are potent central nervous system neurotoxins. *Proceedings of the National Academy of Sciences of the United States of America, 95,* 6448–6453. doi:10.1073/pnas.95.11.6448

Lu, T., Pan, Y., Kao, S. Y., Li, C., Kohane, I., Chan, J., & Yankner, B. A. (2004, June 9). Gene regulation and DNA damage in the aging human brain. *Nature, 429,* 883–891. doi:10.1038/nature02661

Marín-Burgin, A., & Schinder, A. F. (2012). Requirement of adult-born neurons for hippocampus-dependent learning. *Behavioral Brain Research, 227,* 391–399. doi:10.1016/j.bbr.2011.07.001

Miller, M. C., Tavares, R., Johanson, C. E., Hovanesian, V., Donahue, J. E., Gonzalez, L., . . . Stopa, E. G. (2008). Hippocampal RAGE immunoreactivity in early and advanced Alzheimer's disease. *Brain Research, 1230,* 273–280. doi:10.1016/j.brainres.2008.06.124

Ming, G. L., & Song, H. (2011). Adult neurogenesis in the mammalian brain: Significant answers and significant questions. *Neuron, 70,* 687–702. doi:10.1016/j.neuron.2011.05.001

Mucke, L., Masliah, E., & Yu, G.-Q., Mallory, M., Rockenstein, E. M., Tatsuno, G., . . . McConlogue, L. (2000). High-level neuronal expression of $A\beta_1$–42 in wild-type human amyloid protein precursor transgenic mice: Synaptotoxicity without plaque formation. *Journal of Neuroscience, 20,* 4050–4058.

Nadon, N. L. (2007). Animal models in gerontology research. *International Review of Neurobiology, 81,* 15–27. doi:10.1016/S0074-7742(06)81002-0

National Institute of Aging. (2002). *Alzheimer's disease: Unraveling the mystery*. U.S. Department of Health and Human Services, National Institutes of Health; NIH Publication Number 2002; 02–3782.

Nocon, M., Hiemann, T., Muller-Riemenscneider, F., Thalau, F., Roll, S., & Willich, S. N. (2008). Association of physical activity with all-cause and cardiovascular mortality: A systematic review and meta-analysis, *European Journal of Cardiovascular Prevention & Rehabilitation, 15,* 239–246. doi:10.1097/HJR.0b013e3282f55e09

Nowakowski, R. S., Lewin, S. B., & Miller, M. W. (1989). Bromodeoxyuridine immunohistochemical determination of the lengths of the cell cycle and the DNA-synthetic phase for an anatomically defined population. *Journal of Neurocytology, 18,* 311–318. doi:10.1007/BF01190834

O'Nuallain, B., Freir, D. B., Nicoll, A. J., Risse, E., Ferguson, N., Herron, C. E., . . . Walsh, D. M. (2010). Amyloid β-protein dimers rapidly form stable synaptotoxic protofibrils. *The Journal of Neuroscience, 30,* 14411–14419. doi:10.1523/JNEUROSCI.3537-10.2010

Pascale, C. L., Miller, M. C., Chiu, C., Boylan, M., Caralopoulos, I. N., Gonzalez, L., . . . Silverberg, G. D. (2011). Amyloid-beta transporter expression at the blood-CSF barrier is age dependent. *Fluids and Barriers of the CNS, 8,* 21.

Penzes, P., & VanLeeuwen, J.-E. (2011). Impaired regulation of synaptic actin cytoskeleton in Alzheimer's disease. *Brain Research Reviews, 67,* 184–192. doi:10.1016/j.brainresrev.2011.01.003

Price, J. L., Davis, P., Morris, J., & White, D. (1991). The distribution of tangles, plaques, and related immunohistochemical markers in healthy aging and Alzheimer's disease. *Neurobiology of Aging, 12,* 295–312. doi:10.1016/0197-4580(91)90006-6

Querfurth, H. W., & LaFerla, F. M. (2010). Alzheimer's disease. *New England Journal of Medicine, 362,* 329–344. doi:10.1056/NEJMra0909142

Salthouse, T. A. (2000). Aging and measures of processing speed. *Biological Psychology, 54,* 35–54. doi:10.1016/S0301-0511(00)00052-1

Schmidt, A. M., Hasu, M., Popov, D., Zhang, J. H., Chen, J., Yan, S. D., . . . Costache, G. (1994). Receptor for advanced glycation and end products (AGEs) has a central role in vessel wall interactions and gene activation in response to circulating AGE proteins. *Proceedings of the National Academy of Sciences of the United States of America, 91,* 8807–8811.

Selkoe, D. J. (2002, October 25). Alzheimer's disease is a synaptic failure. *Science, 298,* 789–791. doi:10.1126/science.1074069

Shaffer, J. P. (1986). Modified sequentially rejective multiple test procedures. *Journal of the American Statistical Association, 81,* 826–831. doi:10.1080/01621459.1986.10478341

Shruster, A., Eldar-Finkelman, H., Melamed, E., & Offen, D. (2011). Wnt signaling pathway overcomes the disruption of neuronal differentiation of neural progenitor cells induced by oligomeric amyloid β-peptide. *Journal of Neurochemistry, 116,* 522–529. doi:10.1111/j.1471-4159.2010.07131.x

Sidman, R. L. (1970). Autoradiographic methods and principles for study of the nervous system with thymidine-H3. In W. J. H. Nauta & S. O. E. Ebbesson (Eds.), *Contemporary research methods in neuroanatomy* (pp. 252–274). New York, NY: Springer.

Silverberg, G. D., Miller, M. C., Messier, A. A., Majmudar, S., Machan, J. T., Donahue, J. E., . . . Johanson, C. E. (2010a). Amyloid deposition and influx transporter expression at the blood-brain barrier increase in normal aging. *Journal of Neuropathology and Experimental Neurology, 69,* 98–108. doi:10.1097/NEN.0b013e3181c8ad2f

Silverberg, G. D., Miller, M. C., Messier, A. A., Majmudar, S. S., Machan, J. T., Donahue, J. E., . . . Johanson, C. E. (2010b). Amyloid efflux transporter expression at the blood-brain barrier declines in normal aging. *Journal of Neuropathology and Experimental Neurology, 69,* 1034–1043. doi:10.1097/NEN.0b013e3181f46e25

Taupin, P. (2007). BrdU immunohistochemistry for studying adult neurogenesis: Paradigms, pitfalls, limitations, and validation. *Brain Research Reviews, 53,* 198–214. doi:10.1016/j.brainresrev.2006.08.002

Turturro, A., Witt, W. W., Lewis, S., Hess, B. S., Lipman, R. D., & Hart, R. W. (1999). Growth curves and survival characteristics of the animals used in the biomarkers of aging program. *The Journals of Gerontology: Series A: Biological Sciences and Medical Sciences, 54,* B492–B501.

van der Staay, F. J. (2006). Animal models of behavioral dysfunctions: Basic concepts and classifications, and an evaluation strategy. *Brain Research Reviews, 52,* 131–159.

van der Staay, F. J., Arndt, S. S., & Nordquist, R. E. (2009). Evaluation of animal models of neurobehavioral disorders. *Behavioral and Brain Functions, 5,* 11. doi:10.1186/1744-9081-5-11

Walsh, D. M., Klyubin, I., Fadeeva, J. V., Cullen, W. K., Anwyl, R., Wolfe, M. S., . . . Sekoe, D. J. (2002, April 4). Naturally secreted oligomers of amyloid beta protein potently inhibit hippocampal long-term potentiation in vivo. *Nature, 416,* 535–539. doi:10.1038/416535a

Wicklund, L., Leão, R. N., Strömberg, A.-M., Mousavi, M., Hovatta, O., Nordberg, A., & Marutle, A. (2010). β-Amyloid 1–42 oligomers impair function of human embryonic stem cell-derived forebrain cholinergic neurons. *PLoS One, 5,* e15600. doi:10.1371/journal.pone.0015600

Witton, J., Brown, J. T., Jones, M. W., & Randall, A. D. (2010). Altered synaptic plasticity in the mossy fibre pathway of transgenic mice expressing mutant amyloid precursor protein. *Molecular Brain, 3,* 32. doi:10.1186/1756-6606-3-32

Wood, N. I., Glynn, D., & Morton, A. J. (2011). "Brain training" improves cognitive performance and survival in a transgenic mouse model of Huntington's disease. *Neurobiology of Disease, 42,* 427–437. doi:10.1016/j.nbd.2011.02.005

Yankner, B. A., Lu, T., & Loerch, P. (2008). The aging brain. *Annual Review of Pathology, 3,* 41–66. doi:10.1146/annurev.pathmechdis.2.010506.092044

Zlokovic, B. V., Yamada, S., Holtzman, D., Ghiso, J., & Frangione, B. (2000). Clearance of amyloid beta-peptide from brain: Transport or metabolism? *Nature Medicine, 6,* 718–719. doi:10.1038/77397

Received August 12, 2013
Revision received December 23, 2013
Accepted February 18, 2014 ■